THE JOURNAL OF BIOLOGICAL CHEMISTRY VOL. 291, NO. 26, pp. 13571–13579, June 24, 2016

The Globular Tail Domain of Myosin-5a Functions as a Dimer in Regulating the Motor Activity*

Received for publication, February 26, 2016, and in revised form, April 27, 2016 Published, JBC Papers in Press, April 28, 2016, DOI 10.1074/jbc.M116.724328

Wen-Bo Zhang[‡§], **Lin-Lin Yao**[‡], **and Xiang-dong Li**[‡1]

From the [‡]*Group of Cell Motility and Muscle Contraction, State Key Laboratory of Integrated Management of Pest Insects and Rodents, Institute of Zoology, Chinese Academy of Sciences, Beijing 100101, China and the* [§]*University of Chinese Academy of Sciences, Beijing 100049, China*

Myosin-5a contains two heavy chains, which are dimerized via the coiled-coil regions. Thus, myosin-5a comprises two heads and two globular tail domains (GTDs). The GTD is the inhibitory domain that binds to the head and inhibits its motor function. Although the two-headed structure is essential for the processive movement of myosin-5a along actin filaments, little is known about the role of GTD dimerization. Here, we investigated the effect of GTD dimerization on its inhibitory activity. We found that the potent inhibitory activity of the GTD is dependent on its dimerization by the preceding coiled-coil regions, indicating synergistic interactions between the two GTDs and the two heads of myosin-5a. Moreover, we found that alanine mutations of the two conserved basic residues at N-terminal extension of the GTD not only weaken the inhibitory activity of the GTD but also enhance the activation of myosin-5a by its cargo-binding protein melanophilin (Mlph). These results are consistent with the GTD forming a head to head dimer, in which the N-terminal extension of the GTD interacts with the Mlph-binding site in the counterpart GTD. The Mlph-binding site at the GTD-GTD interface must be exposed prior to the binding of Mlph. We therefore propose that the inhibited Myo5a is equilibrated between the folded state, in which the Mlph-binding site is buried, and the preactivated state, in which the Mlph-binding site is exposed, and that Mlph is able to bind to the Myo5a in preactivated state and activates its motor function.

Class V myosin (Myo5),[2] so far the best characterized unconventional myosin, is involved in transport of organelles along actin filaments. Vertebrates express three types of Myo5: Myo5a, Myo5b, and Myo5c (1–3). Among them, Myo5a has been subjected to extensive study.

Myo5a has two heavy chains, each containing an N-terminal motor domain, six IQ motifs that act as the binding sites for calmodulin (CaM) or CaM-like light chains, the proximal tail containing several segments of coiled-coils that dimerize the heavy chain, and the distal tail that forms the globular tail domain (GTD). Because the heavy chain of Myo5a is dimerized through the coiled-coil segments in the proximal tail, Myo5a comprises two heads and the two GTDs. Although it is well established that the two-headed structure is essential for the processive movement of Myo5a along actin filaments, little is known about the roles of GTD dimerization.

The GTD is the inhibitory domain, which interacts with the head of Myo5a and inhibits its motor function. The GTD inhibition can be reversed by Ca^{2+} and cargo-binding proteins (4–10). Similar to Myo5a, vertebrate Myo5b and Myo5c are also inhibited by the GTD in a Ca^{2+}-dependent manner (11, 12), indicating that the tail inhibition mechanism is conserved in all three types of vertebrate Myo5.

Myo5a tail not only plays an inhibitory role but also functions as the binding site for the cargo-binding proteins. In melanocytes, Myo5a tail interacts with its cargo-binding protein melanophilin (Mlph), which associates with melanosome via Rab27a (13–15). Mlph contains two independent Myo5a-binding regions: the exon F-binding domain (EFBD) and the GTD-binding domain (GTBD). The EFBD interacts with the melanocyte-specific exon F region in the Myo5a tail, and the GTBD interacts with the GTD of Myo5a (13, 16, 17). We previously have shown that Mlph is able to stimulate the ATPase activity of Myo5a (15). Quite recently, we demonstrated that Mlph-GTBDP, a 26-amino acid-long peptide within the GTBD of Mlph, is sufficient for activating Myo5a motor function (18). Because the GTD uses two distinct, nonoverlapping regions to interact with Mlph-GTBDP and the head of Myo5a (19, 20), we proposed that the GTD is an allosteric protein. In other words, Mlph-GTBDP allosterically inhibits the interaction between the GTD and head of Myo5a, thereby activating its motor function (18). Those studies indicate that the tail, particularly the GTD, plays a central role in regulating Myo5a motor function.

Our previous studies have shown that the GST-tagged GTD displays stronger inhibition of Myo5a-HMM than the His-tagged GTD (7, 10, 21). Because the His-tagged GTD is mostly monomeric (10) and the GST-tagged GTD is dimeric, it is possible that the two GTDs in the GST-tagged GTD synergistically interact with the two heads of Myo5a-HMM, thus having higher affinity to Myo5a-HMM. In the intact Myo5a molecule, the GTD is preceded by coiled-coil segments that enable the two GTDs to form a homodimer. However, the significance of GTD dimerization in the Myo5a regulation remains to be clarified.

* This work was supported by National Basic Research Program of China Grants 2013CB932802 and 2012CB114102 and the National Natural Science Foundation of China Grants 31171367 and 31470791. The authors declare that they have no conflicts of interest with the contents of this article.

[1] To whom correspondence should be addressed: Institute of Zoology, Chinese Academy of Sciences, Beijing 100101, China. Tel.: 86-10-6480-6015; E-mail: lixd@ioz.ac.cn.

[2] The abbreviations used are: Myo5, class V myosin; CaM, calmodulin; EFBD, exon F binding domain of melanophilin; GTBD, the GTD-binding domain of melanophilin; GTD, globular tail domain of myosin-5a; HMM, heavy meromyosin; Mlph, melanophilin; WB, wash buffer.

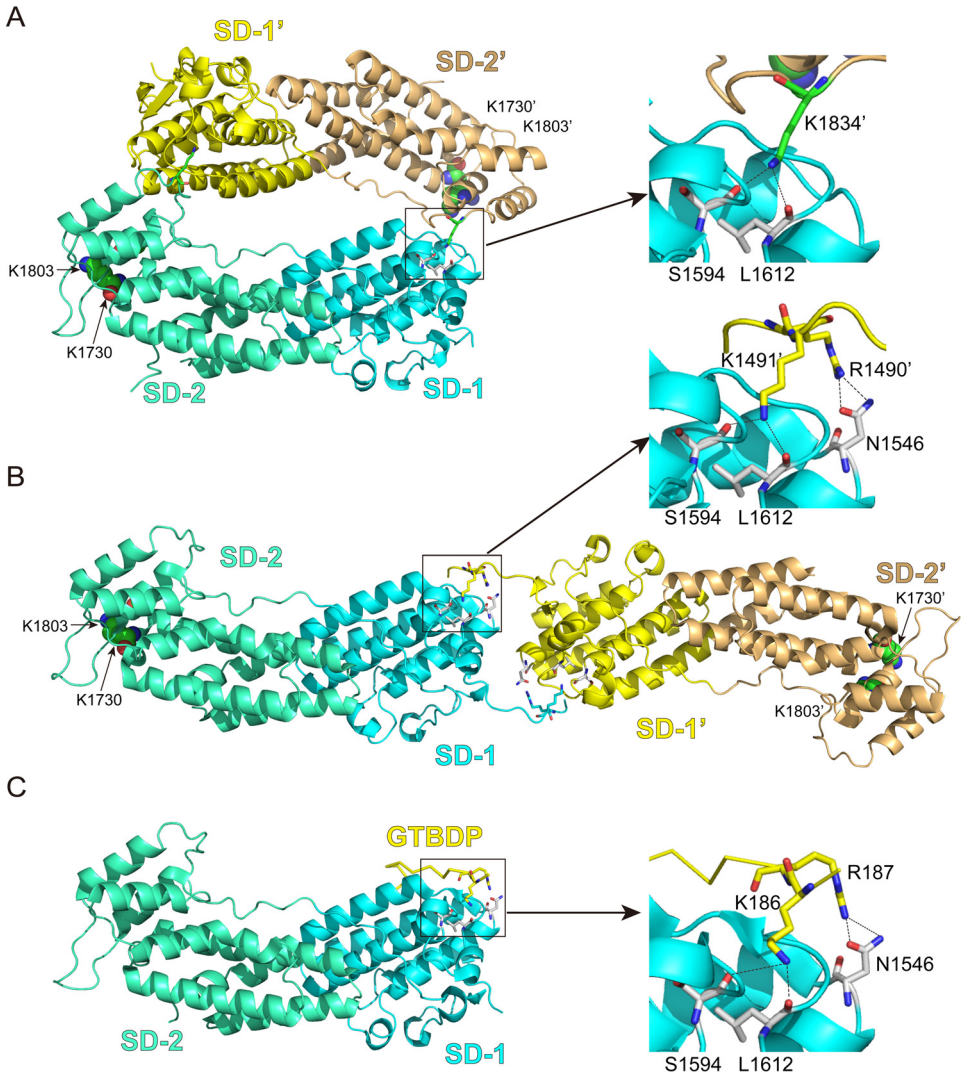

FIGURE 1. **The interactions between the GTD dimer and between Myo5a-GTD and Mlph-GTBDP.** *A*, cartoon representation of the Myo5a-GTD structure (Protein Data Bank code 3WB8) showing a head to tail dimer. There are four putative dimers in the crystal structure of mouse Myo5a-GTD, and only one dimer (chains a and c) is shown here. *B*, cartoon representation of Myo5b-GTD structure (Protein Data Bank code 4J5M) showing a head to head dimer. *C*, cartoon representation of the Myo5a-GTD·Mlph-GTBDP complex structure (Protein Data Bank code 4LX2). *SD-1* and *SD-2* indicate subdomains 1 and 2 of the GTD, respectively. *Sticks* show the residues at the GTD-GTD interface and the interface between Myo5a-GTD and Mlph-GTBDP. *Spheres* show the two conserved basic residues Lys^{1730} and Lys^{1803}, which are essential for inhibiting motor function (7). In the head to tail model of the GTD dimer, the distances between the two Lys^{1730} and between the two Lys^{1803} are 79 and 66 Å, respectively. In the head to head model of the GTD dimer, the distances between the two Lys^{1730} and between the two Lys^{1803} are 153 and 142 Å, respectively. For clarity, all residue numbers refer to the melanocyte isoform of Myo5a (see "Experimental Procedures" for details).

Interestingly, in three of four crystal structures of Myo5a-GTD thus far solved (19, 20, 22, 23), Myo5a-GTD seems to forms a "head to tail" dimer (Fig. 1*A*). On the other hand, Houdusse and co-workers (20) proposed a "head to head" model for GTD dimer that is formed via the binding of the N-terminal extension of one GTD with the symmetry-related GTD (Fig. 1*B*). It is not known which type of GTD dimer is formed in the intact Myo5a. Intriguingly, the putative GTD-GTD interface, in either the head to tail model or the head to head model, is overlapped with the Mlph-GTBDP binding site (Fig. 1*C*), suggesting that the GTD dimerization might prevent Mlph-GTBDP from binding.

In the present study, we investigated the role of GTD dimerization on its inhibitory function by analyzing the inhibitory activity of Myo5a tail containing the GTD and variously truncated coiled-coil segments. We found that the potent inhibitory activity of the GTD is dependent on its dimerization by the coiled-coil regions. Consistent with the head to head model of the GTD dimer, we found that the mutation of two conserved basic residues at the N-terminal extension of the GTD not only weakens the inhibitory activity of the GTD but also enhances the activation of Myo5a by Mlph-GTBDP.

Experimental Procedures

Materials—Restriction enzymes and modifying enzymes were purchased from New England Biolabs (Beverly, MA), unless indicated otherwise. Actin was prepared from rabbit skeletal muscle acetone powder according to Spudich and Watt (24). Nickel-nitrilotriacetic acid-agarose was purchased from Qiagen. Anti-FLAG M2 affinity gel, phosphoenol pyruvate, 2,4-dinitrophenyl-hydrazine, and pyruvate kinase were from Sigma. GSH-Sepharose 4 Fast Flow was from GE Healthcare.

FLAG peptide (DYKDDDDK) was synthesized by Augct Co. (Beijing, China). Oligonucleotides were synthesized by Invitrogen.

Mlph-GTBDP, a synthesized peptide containing residues 176–201 of Mlph and a C-terminal tyrosine (for accurate concentration determination), was prepared as described (18). GST-Mlph-GTBDP, a GST fusion protein of Mlph-GTBDP, was expressed in *Escherichia coli* and purified as described (18).

Myo5a Constructs—All Myo5a constructs in this study were created from a melanocyte isoform of Myo5a cDNA (25). Myo5a-HMM (amino acids 1–1234) with N-terminal His tag and FLAG tag was prepared as described previously (10). Full-length Myo5a mutant, *i.e.* Myo5a-FL-R1490A/K1491A, was created by site-directed mutagenesis. All Myo5a constructs containing the motor domain were expressed in Sf9 insect cells and purified by anti-FLAG M2 affinity chromatography (7).

Four truncated Myo5a tail constructs containing an N-terminal His tag were created, including Myo5a-T1235 (Pro^{1235}–Val^{1877}), Myo5a-T1344 (Arg^{1344}–Val^{1877}), Myo5a-T1432 (Lys^{1432}–Val^{1877}), and Myo5a-GTD (Gly^{1468}–Val^{1877}). The cDNAs of truncated Myo5a tail were subcloned into pET30a (Amersham Biosciences) using BamHI and XhoI sites. Point mutations were introduced by QuikChange site-directed mutagenesis and standard molecular biological techniques. His-tagged Myo5a tail constructs were expressed in BL21(DE3) *E. coli* and purified by nickel-nitrilotriacetic acid-agarose affinity chromatography using standard procedures. GST-tagged Myo5a-GTD was prepared as described (7). All purified Myo5a tail proteins were dialyzed against 10 mM Tris-HCl (pH 7.5), 0.2 M NaCl, and 1 mM DTT.

The concentrations of the purified Myo5a tail were determined by absorbance at 280 nm, using the following molar extinction coefficients: 48,040 liters·mol^{-1}·cm^{-1}, His-Myo5a-T1235; 37,230 liters·mol^{-1}·cm^{-1}, His-Myo5a-T1344; 30,830 liters·mol^{-1}·cm^{-1}, His-Myo5a-T1432 and His-Myo5a-GTD; and 71,990 liters·mol^{-1}·cm^{-1}, GST-Myo5a-GTD. Note that the concentrations of Myo5a constructs in this study refer to the mole of polypeptide chain, regardless of their dimerization states.

In this study, the residue numbers of Myo5a refer to a melanocyte isoform of Myo5a, which contains the alternatively spliced exons D and F but lacks exon B (25). In most other publications, the residue numbers of Myo5a refer to the isoform of Myo5a (GenBank™ accession no. X57377) containing exons B and F but lacking exon D. Therefore, the present construct is 24 residues longer than that in most publications. The residue numbers in this study and the corresponding residue numbers (in parentheses) in other publications are Arg^{1490} (1466), Lys^{1491} (1467), Asn^{1546} (1522), Ser^{1594} (1570), Leu^{1612} (1588), Lys^{1730} (1706), Lys^{1803} (1779), and Lys^{1834} (1810).

Size Exclusion Chromatography of Myo5a Tail—Myo5a tail protein (1–2 μg/μl, 200 μl) was applied to a Superdex G200 size exclusion column (10 × 300 mm; GE Healthcare) preequilibrated with 200 mM NaCl, 1 mM DTT, 10 mM Tris-HCl (pH 7.5) and eluted with the same solution at a flow rate of 0.5 ml/min. Lysozyme (14.4 kDa), carbonic anhydrase (29 kDa), BSA (66 kDa), and IgG (150 kDa) were used as protein standards under the same chromatography conditions as the target proteins. The peaks of target proteins and protein standards were confirmed by SDS-PAGE. The molecular masses of the target proteins were calculated using linear regression.

ATPase Assay—The ATPase activity was measured at 25 °C in a plate-based, ATP regeneration system as described previously (7). The detailed assay conditions are described in each figure legends. The dissociation constants (K_d) of Myo5a tail to Myo5a-HMM were obtained by a hyperbolic fit using Kaleidagraph software (Synergy Software, Reading, PA).

GST Pulldown Assay—To detect the interaction between Mlph-GTBDP and Myo5a-FL, GSH-Sepharose (20 μl) was mixed with 100 μl of 1 μM GST-Mlph-GTBDP and 1 μM FLAG-tagged Myo5a-FL wild type or R1490A/K1491A in wash buffer (WB; 5 mM Tris-HCl, pH 7.5, 200 mM NaCl, 1 mM DTT, and 1 mM EGTA) and then incubated at 4 °C with rotation for 2 h. After brief centrifugation (2,000 × *g* for 10 s), the supernatants were discarded, and the pellets were washed with 200 μl of WB for three times to remove the unbound proteins. The bound proteins were eluted by 45 μl of 10 mM GSH in WB. The eluted proteins were subjected to SDS-PAGE (4–20%) and detected by Western blot using HRP-conjugated anti-FLAG antibody (Sigma-Aldrich) or anti-GST antibody and HRP-conjugated goat anti-mouse second antibody.

To examine the effect of R1490A/K1491A mutation of His-Myo5a-T1344 on the interaction with Mlph-GTBDP, we performed competition pulldown assay. We mixed 5 μM His-Myo5a-T1235 and 5 μM His-Myo5a-T1344 wild type or R1490A/K1491A with 4 μM GST-Mlph-GTBDP in WB (5 mM Tris-HCl, pH 7.5, 200 mM NaCl, 1 mM DTT, and 1 mM EGTA). Above mixture (100 μl) was then mixed with 15 μl of GSH-Sepharose beads and incubated at 4 °C with rotation for 2 h. The unbound proteins were removed by washing with 200 μl of WB four times, and the bound proteins were then eluted twice with 20 μl of 10 mM GSH in WB. The eluted proteins were separated by SDS-PAGE (4–20%) and visualized by Coomassie Blue staining. The amounts of pulled down proteins were quantified using ImageJ (version 1.42Q), and their molar ratios were calculated on the basis of their molecular masses.

Results

Dimerization of Myo5a Tail Enhances the Affinity to Myo5a-HMM—The two GTDs in intact Myo5a form a dimer via the coiled-coils in the proximal tail. To investigate the role of GTD dimerization on its inhibitory activity, we created a number of Myo5a tail constructs containing the GTD and different length of coiled-coil (Fig. 2*A*). To facilitate purification, a His tag was attached to the N-terminal of those constructs. Those Myo5a tail constructs were overexpressed in *E. coli* and purified by nickel-nitrilotriacetic acid-agarose affinity chromatography. The apparent molecular masses of Myo5a tail constructs in SDS-PAGE agree well with the calculated values based on their sequences (Fig. 2*B*).

To determine the inhibitory activity of Myo5a tail constructs, we measured the actin-activated ATPase activity (hereafter referred to as ATPase activity) of Myo5a-HMM in the presence of Myo5a tail. Although all Myo5a tail constructs inhibited the ATPase activity of Myo5a-HMM, the Myo5a tail constructs containing longer coiled-coil, including His-Myo5a-T1235 and

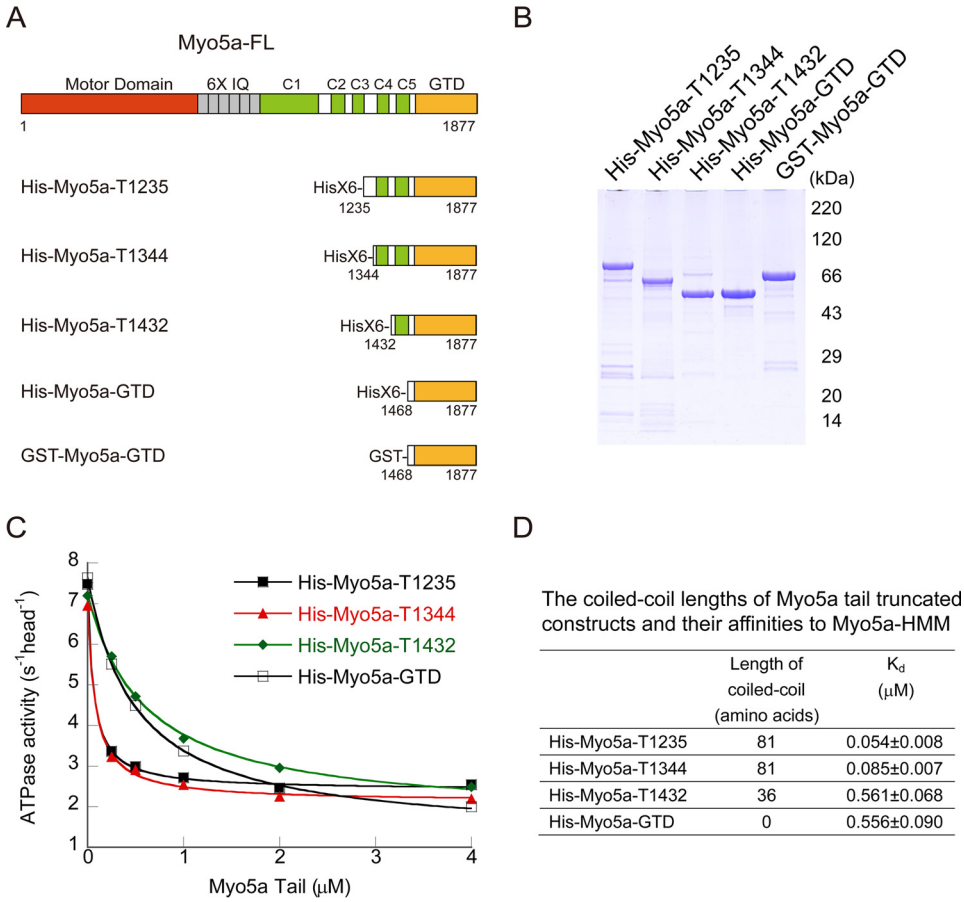

The coiled-coil lengths of Myo5a tail truncated constructs and their affinities to Myo5a-HMM

	Length of coiled-coil (amino acids)	K_d (μM)
His-Myo5a-T1235	81	0.054±0.008
His-Myo5a-T1344	81	0.085±0.007
His-Myo5a-T1432	36	0.561±0.068
His-Myo5a-GTD	0	0.556±0.090

FIGURE 2. **Shortening of coiled-coil in the Myo5a tail decreases its affinity to Myo5a-HMM.** *A*, diagram of Myo5a structure and Myo5 tail truncation constructs. The coiled-coils were predicted by an online tool (Paircoil). The residue numbers in this study refer to a melanocyte isoform of Myo5a, which is 24 residues longer than that used in most publications. See "Experimental Procedures" for the corresponding residues numbers in most publications. *B*, SDS-PAGE (4–20%) of purified Myo5a tail proteins. *C*, the ATPase activity of Myo5a-HMM in the presence of Myo5a tail with different length of coiled-coil. The ATPase activity of Myo5a-HMM was measured in a solution containing 20 mM MOPS-KOH (pH 7.0), 100 mM NaCl, 1 mM $MgCl_2$, 1 mM DTT, 0.25 mg/ml BSA, 12 μM CaM, 0.5 mM ATP, 2.5 mM phosphoenol pyruvate, 20 units/ml pyruvate kinase, 40 μM actin, 1 mM EGTA, 0.03–0.05 μM Myo5a-HMM, and various concentrations of Myo5a tail. The K_d of Myo5a tail to Myo5a-HMM was obtained by a hyperbolic fit. *D*, the calculated K_d of Myo5a tail to Myo5a-HMM. The K_d values are means ± S.D. from three independent assays of two protein preparations.

His-Myo5a-T1344, had higher affinity to Myo5a-HMM than those containing shorter coiled-coil, including His-Myo5a-T1432 and His-Myo5a-GTD (Fig. 2, *C* and *D*). These results indicate that the coiled-coil segment of 1344–1432 plays a critical role in potent interaction between Myo5a tail and Myo5a-HMM.

The dissociation constants (K_d) of His-Myo5a-T1235 and His-Myo5a-T1344 to Myo5a-HMM are similar to that of GST-Myo5a-GTD, a dimerized GTD (7). We thus expected that, similar to GST-Myo5a-GTD, His-Myo5a-T1235 and His-Myo5a-T1344 are dimer, whereas His-Myo5a-T1432 and His-Myo5a-GTD are monomer. To test this possibility, we estimated the apparent molecular masses of Myo5a tail constructs using size exclusive chromatography (Fig. 3). The apparent molecular masses of His-Myo5a-T1344, -T1432, and His-Myo5a-GTD were 162.1, 80.1, and 80.3 kDa, respectively, indicating that His-Myo5a-T1344 forms a dimer and that His-Myo5a-T1432 and His-Myo5a-GTD are mostly monomeric. As the control, GST-Myo5a-GTD had an apparent molecular mass of 154.9 kDa in size exclusive chromatography, consistent with its dimerization. These results indicate that the coiled-coil segment of 1344–1432 is essential for the dimerization of Myo5a-GTD, which is required for potent inhibition of Myo5a motor function.

Two Conserved Basic Residues in the N-terminal Extension of the GTD Are Essential for Potent Inhibition of Myo5a-HMM—Although the GTD dimerization is essential for the potent interaction between the GTD and the head of Myo5a, the structure of GTD dimer has not been established. Crystal structures of Myo5a-GTD and Myo5b-GTD reveal two models of GTD dimer: the head to tail dimer and the head to head dimer (Fig. 1, *A* and *B*).

Intriguingly, the putative GTD-GTD interface in either models is overlapped with the Mlph-GTBDP binding site (Fig. 1*C*). In addition to hydrophobic interactions, Mlph-GTBDP forms extensive hydrogen bonds with Myo5a-GTD, including the hydrogen bonds between the side chains of Lys^{186} in Mlph and the carbonyl group of Leu^{1612} and the side chains of Ser^{1594} in Myo5a-GTD and that between the side chain of Arg^{187} in Mlph and the side chains of Asn^{1546} in Myo5a-GTD (19, 20).

In the head to tail model of Myo5a-GTD dimer, basic residue Lys^{1834} occupies the same position as Lys^{186} of Mlph in the Myo5a-GTD·Mlph-GTBDP complex. Similar to that of Lys^{186} of Mlph, the side chain of Lys^{1834} in one GTD interacts with the

A

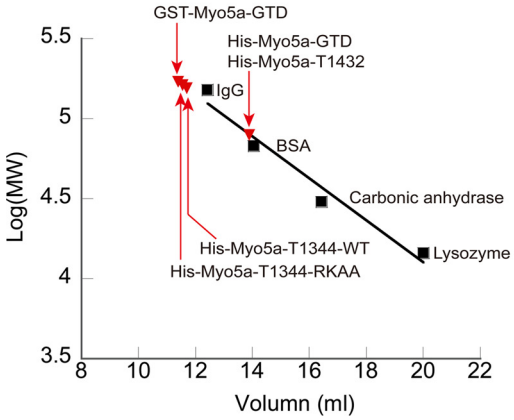

B

The molecular masses of Myo5a tail constructs estimated from size-exclusive chromatography

Myo5a Tail construct	Theoretic MW (kDa)		Apparent MW (kDa)
	Monomer	Dimer	
His-Myo5a-GTD	50.1	100.2	80.3
GST-Myo5a-GTD	73.2	146.4	154.9
His-Myo5a-T1432	56.6	113.2	80.1
His-Myo5a-T1344 -WT	67.1	134.2	162.1
His-Myo5a-T1344 - RKAA	67.0	134.0	170.1

FIGURE 3. **Size exclusive chromatography of Myo5a tail constructs.** *A*, Superdex G200 size exclusion chromatography of the purified Myo5a tail constructs. *Black squares* indicate the elution peaks of each standard proteins. *Red triangles* indicate the elution peaks of each Myo5a tail constructs. The void volume of the column was 7.7 ml. *B*, the theoretical and apparent molecular masses of Myo5a tail constructs. The theoretical molecular masses were calculated on the basis of the amino acid composition of Myo5 tail. The apparent molecular masses were estimated from size exclusion chromatography. *RKAA*, R1490A/K1491A.

carbonyl group of Leu^{1612} in the counterpart GTD (Fig. 1*A*). On the other hand, in the head to head model of Myo5b-GTD dimer, the two conserved basic residues Arg^{1490} (Arg^{1461} of Myo5b) and Lys^{1491} (Lys^{1462} of Myo5b) at the N-terminal extension of one GTD occupy the same positions as Arg^{187} and Lys^{186} of Mlph in Myo5a-GTD·Mlph-GTBDP complex (Fig. 1*B*). The side chain of Arg^{1490} makes hydrogen bond with Asn^{1546} (Asn^{1516} of Myo5b), and the side chain of Lys^{1491} makes hydrogen bonds with Leu^{1612} and Ser^{1594} (Leu^{1582} and Ser^{1564} of Myo5b, respectively) in the counterpart GTD.

To determine the role of the basic residues located in the putative GTD-GTD interface, we mutated those basic residues to alanine and examined the inhibitory activity of GST-Myo5a-GTD mutants. As shown in Fig. 4*A*, both R1490A and K1491A mutations strongly decreased the affinity of GST-Myo5a-GTD to Myo5a-HMM, and R1490A/K1491A double mutation decreased the affinity at the same extent as the single mutations. In contrast, K1834A mutation had little effect on the inhibitory activity of GST-Myo5a-GTD (Fig. 4, *A* and *D*). These results indicate that both Arg^{1490} and Lys^{1491} are essential for the potent interaction between the GTD dimer and Myo5a-HMM, consistent with the head to head model of GTD dimer.

To further investigate the role of Arg^{1490} and Lys^{1491} on the GTD, which is dimerized through its native coiled-coil, we introduced R1490A and K1491A mutations in His-Myo5a-T1344. Similar to the effects on GST-Myo5a-GTD, both R1490A and K1491A single mutations, as well as R1490A/K1491A double mutations, strongly decreased the affinity of His-Myo5a-T1344 to Myo5a-HMM (Fig. 4, *B* and *D*). To determine whether R1490A/K1491A mutations affect the dimerization of His-Myo5a-T1344, we estimated the molecular mass of His-Myo5a-T1344-R1490A/K1491A using size exclusion chromatography (Fig. 3). The apparent molecular mass of His-Myo5a-T1344-R1490A/K1491A was similar to that of the wild type, indicating that R1490A/K1491A mutations do not affect GTD dimerization in His-Myo5a-T1344. It is likely that R1490A/K1491A mutation disrupts the proper interaction between the two GTDs of His-Myo5a-T1344, thus abrogating the synergistic interaction between the two GTDs and the two heads of Myo5a-HMM.

To investigate whether Arg^{1490} and Lys^{1491} also play a role in the inhibition of Myo5a-HMM by monomeric GTD, we mutated those residues to alanine in His-Myo5a-GTD. Neither the single mutations (R1490A or K1491A) nor the double mutation (R1490A/K1491A) significantly affected the affinity of His-Myo5a-GTD to Myo5a-HMM (Fig. 4, *C* and *D*), indicating that Arg^{1490} and Lys^{1491} play a role in dimeric GTD but not in monomeric GTD.

R1490A/K1491A Mutation Weakens the Tail Inhibition of Myo5a and Enhances the Activation by Mlph-GTBDP—To directly investigate the roles of Arg^{1490} and Lys^{1491} on the regulation of Myo5a, we introduced R1490A/K1491A mutations in full-length Myo5a (Myo5a-FL). Comparing with the wild type, Myo5a-FL-R1490A/K1491A had a normal level of ATPase activity in pCa4 conditions but an elevated ATPase activity in EGTA conditions (Fig. 5*A*), indicating that both residues are required for stabilization of the inhibited state of Myo5a.

Because the GTD-GTD interface in head to head model overlaps the binding site for Mlph-GTBDP, the interaction between the two GTDs is likely to reduce the interaction between the GTD and Mlph-GTBDP. We thus expected that R1490A/K1491A mutation will increase the interaction between the GTD and Mlph-GTBDP and enhance the activation of Myo5a-FL by Mlph-GTBDP. Indeed, R1490A/K1491A mutation enhanced the activation of Myo5a-FL ATPase activity by Mlph-GTBDP, with apparent K_d decreasing from 32.6 ± 8.2 μM for wild type and 7.3 ± 0.9 μM for the mutant (Fig. 5*B*). Note that a relatively high concentration of salt (*i.e.* 200 mM NaCl) is needed for the activation of Myo5a-FL by Mlph-GTBDP and that increasing the salt concentration reduces the maximal ATPase activity.

To access the effects of R1490A/K1491A mutation on the interaction between Myo5a-FL and Mlph-GTBDP, we performed GST pulldown assay. FLAG-tagged Myo5a-FL was mixed with GST-Mlph-GTBDP and then incubated with GSH-

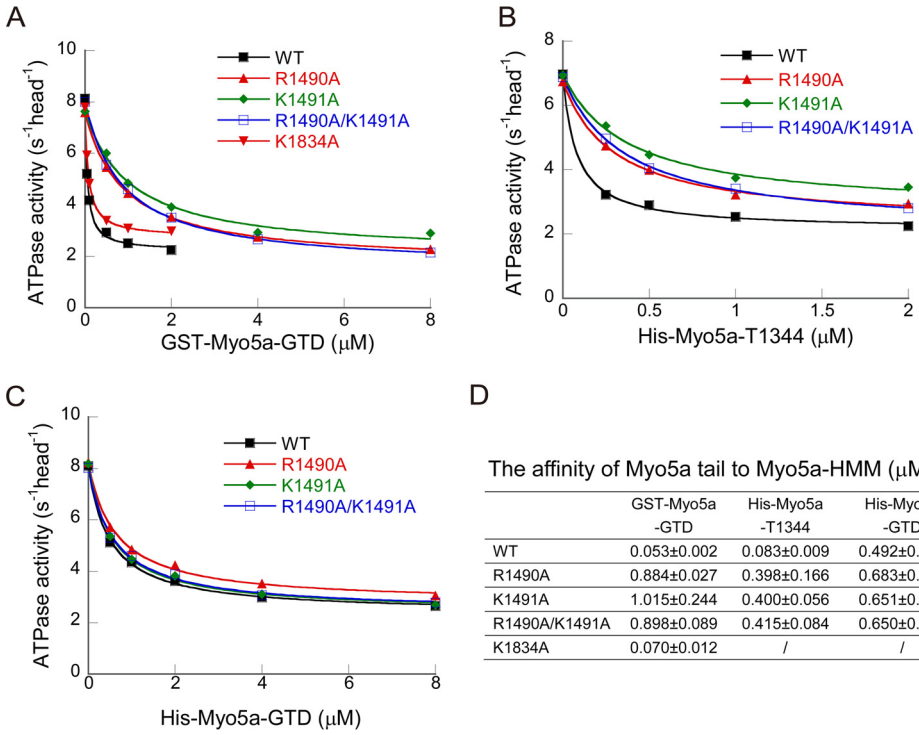

D

The affinity of Myo5a tail to Myo5a-HMM (μM)

	GST-Myo5a -GTD	His-Myo5a -T1344	His-Myo5a -GTD
WT	0.053±0.002	0.083±0.009	0.492±0.070
R1490A	0.884±0.027	0.398±0.166	0.683±0.090
K1491A	1.015±0.244	0.400±0.056	0.651±0.102
R1490A/K1491A	0.898±0.089	0.415±0.084	0.650±0.068
K1834A	0.070±0.012	/	/

FIGURE 4. **Mutation of the conserved basic residues at the GTD-GTD interface of Myo5a GTD dimer decreases the affinity to Myo5a-HMM.** *A–C*, the ATPase activity of Myo5a-HMM was measured in the presence of GST-Myo5a-GTD (*A*), His-Myo5a-T1344 (*B*), or His-Myo5a-GTD (*C*). The ATPase assay was conducted as described in the legend of Fig. 2. *D*, the K_d of Myo5a tail constructs to Myo5a-HMM. The values are means ± S.D. from three independent assays of two protein preparations.

Sepharose. The FLAG-tagged Myo5a-FL and GST-Mlph-GTBDP retained on the GSH-Sepharose beads were analyzed by Western blot (Fig. 5*C*). Consistent with the results of ATPase assay, R1490A/K1491A mutations enhanced the binding of Mlph-GTBDP to Myo5a-FL. The amount of Myo5a-FL R1490A/K1491A mutant pulled down with GST-Mlph-GTBDP was approximately four times as that of the wild type.

We expected that R1490A/K1491A mutation would also enhance the interaction between Myo5a tail and Mlph-GTBDP. Therefore, we performed GST pulldown assay of GST-Mlph-GTBDP with His-Myo5a-T1344 wild type and R1490A/K1491A. Contrary to our expectation, nearly equal amounts of His-Myo5a-T1344 wild type and R1490A/K1491A were pulled down with GST-Mlph-GTBDP.

To more rigorously examine the effect of R1490A/K1491A mutations on the interaction between Mlph-GTBDP and Myo5a Tail, we performed competition GST pulldown assay. Equal moles of His-Myo5a-T1235 and His-Myo5a-T1344 (wild type or R1490A/K1491A mutant) were mixed with GST-Mlph-GTBDP and then pulled down by GSH-Sepharose. The pulled down proteins were analyzed by SDS-PAGE followed by Coomassie Blue staining. Nearly equal moles of His-Myo5a-T1235 and His-Myo5a-T1344 wild type were pulled down (Fig. 5*D*, *first lane*), indicating that both constructs have similar affinity to GST-Mlph-GTBDP. Similar to the wild type, nearly equal moles of His-Myo5a-T1344 R1490A/K1491A mutant and His-Myo5a-T1235 were pulled down with GST-Mlph-GTBDP (Fig. 5*D*). These results indicate that R1490A/K1491A mutation does not affect the interaction between Mlph-GTBDP and Myo5a tail.

Discussion

The Structures of the GTD Dimer and the Inhibited Myo5a—It is well established that the inhibited Myo5a is in a folded, triangular conformation, in which the GTD folds back to interact with the head of Myo5a (4, 7, 8, 10). However, the precise interactions that stabilize the triangular conformation of Myo5a are not known, because the high resolution structure of folded Myo5a has not been solved. In this study, we demonstrated that the interaction between the N-terminal extension of the GTD and the Mlph-GTBDP binding site in the counterpart GTD is essential for potent binding of the GTD dimer to the two heads of Myo5a, indicating that the GTD-GTD interaction stabilizes the triangular conformation of the inhibited Myo5a.

Our results support the head to head model of Myo5a-GTD dimer (20) (Fig. 1*B*). The head to head model of GTD dimer is consistent with the geometry of the triangular conformation of the inhibited Myo5a. We previously showed that the conserved acidic residue Asp^{136} in the motor domain and two basic residues Lys^{1730} and Lys^{1803} in the GTD are essential for the folded inhibited state of Myo5a and proposed the direct interactions between Asp^{136} and Lys^{1730}/Lys^{1803} (7, 26). The distance between the two Asp^{136} in the folded structure of Myo5a (Protein Data Bank code 2DFS) is ~150 Å. In the head to head model of the GTD dimer (Fig. 1*B*), the distances between the two Lys^{1730} and between the two Lys^{1803} are 153 and 142 Å, consistent with the direct interactions between Asp^{136} and Lys^{1730}/Lys^{1803}. On the other hand, in the head to tail model of the GTD dimer (Fig. 1*A*), those distances are 79 and 66 Å,

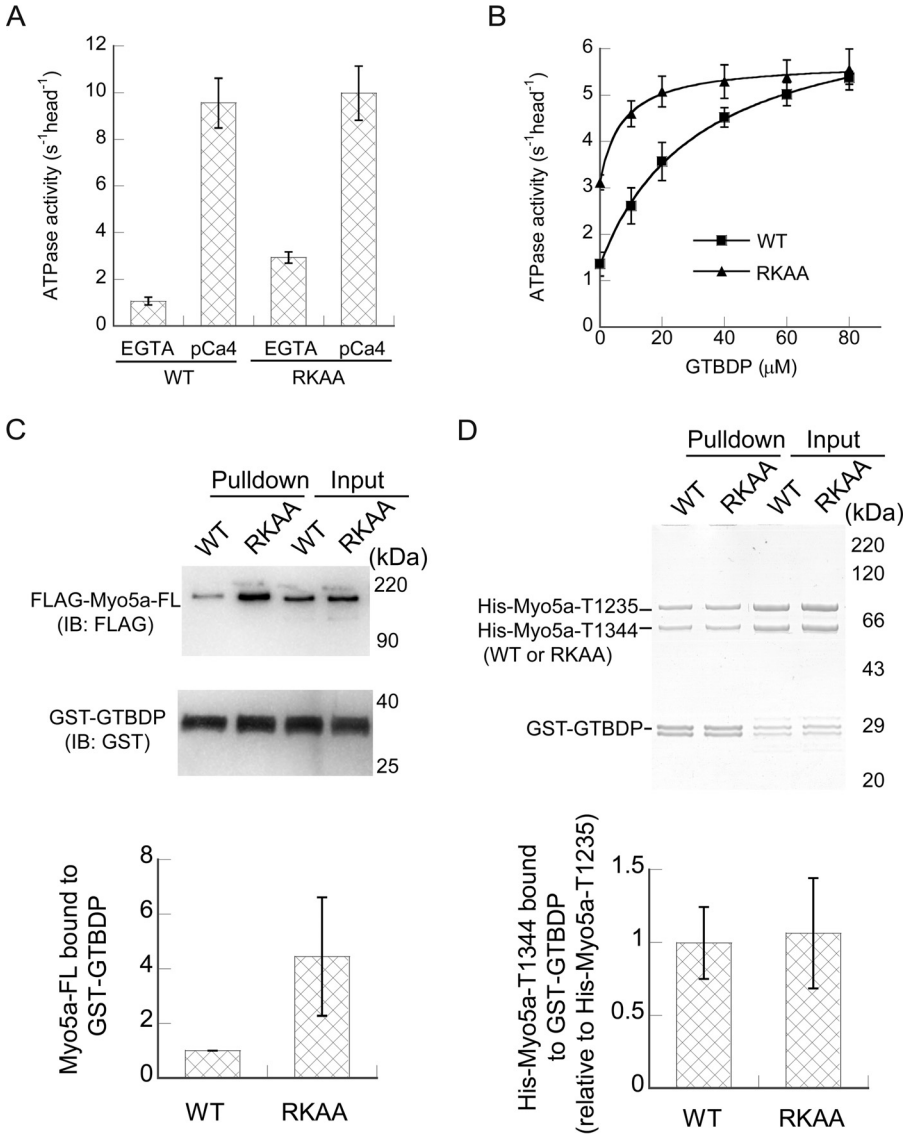

FIGURE 5. **Effects of R1490A/K1491A mutations on the regulation of Myo5a-FL and the activation by Mlph-GTBDP.** *A*, the ATPase activities of Myo5a-FL under EGTA and pCa4 conditions. The ATPase activity of Myo5a-FL was measured in a solution containing 20 mM MOPS-KOH (pH 7.0), 100 mM KCl, 1 mM $MgCl_2$, 1 mM DTT, 0.25 mg/ml BSA, 12 μM CaM, 0.5 mM ATP, 2.5 mM phosphoenol pyruvate, 20 units/ml pyruvate kinase, 40 μM actin, 1 mM EGTA, and 0.02–0.04 μM Myo5a-FL. EGTA (1 mM) was replaced with 0.9 mM EGTA and 1 mM $CaCl_2$ for pCa4 conditions. The values are means ± S.D. from three independent assays of three protein preparations. *B*, stimulation of the ATPase activity of Myo5a-FL by Mlph-GTBDP. The ATPase activity was measured in a solution containing 20 mM MOPS-KOH (pH 7.0), 200 mM NaCl, 1 mM $MgCl_2$, 1 mM DTT, 0.25 mg/ml BSA, 12 μM CaM, 0.5 mM ATP, 2.5 mM phosphoenol pyruvate, 20 units/ml pyruvate kinase, 40 μM actin, 1 mM EGTA, 0.03–0.04 μM Myo5a-FL, and various concentrations of the Mlph-GTBDP. Stimulation of the ATPase activity of Myo5a-FL by Mlph-GTBDP was fit to a hyperbola, defining K_d, the apparent dissociation constants of Mlph-GTBDP to Myo5a-FL, which were 32.6 ± 8.2 μM for wild type and 7.3 ± 0.9 μM for R1490A/K1491A. The values are means ± S.D. from three independent assays of three protein preparations. *C*, GST pulldown of GST-Mlph-GTBDP with FLAG-tagged Myo5a-FL. The pulled down samples and the inputs were analyzed by SDS-PAGE and detected by Western blot using anti-FLAG antibody and anti-GST antibody (*top panel*). The amounts of pulled down Myo5a-FL were quantified using NIH image program. The *bottom panel* shows the means ± S.D. of the amount of pulled down Myo5a-FL (relative to WT) from three independent assays of a single protein preparation. *D*, GST pulldown of GST-Mlph-GTBDP with His-Myo5a-T1235-WT and His-Myo5a-T1344-WT or -RKAA. The pulled down samples were analyzed by SDS-PAGE and detected by Coomassie Blue staining (*top panel*). The amounts of pulled down His-Myo5a-T1235 and His-Myo5a-T1344 were quantified as described under "Experimental Procedures." The *bottom panel* shows the means ± S.D. of the mole of pulled down His-Myo5a-T1344 (relative to His-Myo5a-T1235-WT) from five independent assays of a two protein preparations. *RKAA*, R1490A/K1491A; *IB*, immunoblotting.

respectively, which are much shorter than that between the two Asp^{136} residues.

The triangular conformation of the inhibited Myo5a is likely stabilized by multiple intramolecular interactions, including the interactions between Asp^{136} in the motor domain and Lys^{1730}/Lys^{1803} in the GTD (7), between the C-lobe of CaM bound to IQ1 and the H11-H12 loop of the GTD (18, 21), between the GTD and the C terminus of first coiled-coil (10), and between the two GTDs. The first two interactions seem to be essential for the inhibition by the GTD, because elimination of any of those interactions abolishes the inhibition (7, 18), whereas the last two interactions play an auxiliary role for the inhibition, because elimination of any of those interactions weakens, but not abolishes, the inhibition (10).

Activation of Myo5a by Mlph-GTBDP—The motor function of Myo5a can be stimulated by the cargo-binding protein Mlph via the interaction between Mlph-GTBDP and the GTD of Myo5a (18). Because the GTD uses two distinct, nonoverlap-

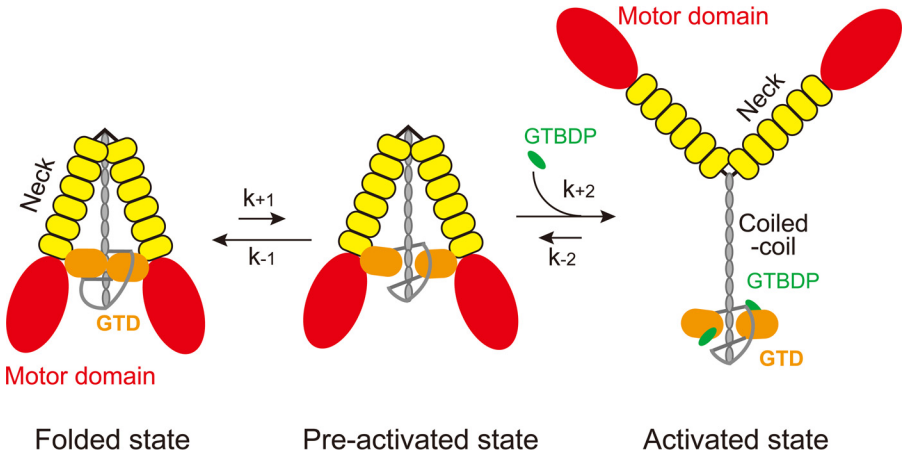

FIGURE 6. **Proposed mechanism for the activation of Myo5a by Mlph-GTBDP.** The inhibited Myo5a molecules are equilibrated between the folded state and the preactivated state. In the folded state, the two GTDs form a head to head dimer via the interaction between the N-terminal extension in one GTD and the Mlph-GTBDP binding site in the counterpart GTD; the GTD dimer interact with the two heads of Myo5a, thus forming a folded, triangular conformation. In the preactivated state, Myo5a also forms a folded, triangular conformation as in the folded state, except that the Mlph-GTBDP binding sites in the GTDs are exposed. Mlph-GTBDP is able to bind to the GTD of Myo5a in preactivated state and allosterically inhibits the binding of GTD to the head, thus inducing the extended conformation and activating the motor function of Myo5a.

ping regions to interact with Mlph-GTBDP and the head of myosin-5a, we proposed that the binding of Mlph-GTBDP to the GTD allosterically inhibits the interaction between the GTD and the head of Myo5a, thereby activating the motor function (18).

In the head to head model of GTD dimer, the GTD-GTD interface overlaps the binding site for Mlph-GTBDP. Similar to Arg^{187} and Lys^{186} of Mlph, the two conserved basic residues Arg^{1490} and Lys^{1491} in the N-terminal extension of one GTD interact with the counterpart GTD (Fig. 1). Thus, the interactions between the two GTDs are predicted to reduce the interaction between the GTD and Mlph-GTBDP (20). Consistently, we found that R1490A/K1491A mutation increases the binding of Mlph-GTBDP to Myo5a-FL and enhances the activation of Myo5a-FL by Mlph-GTBDP. However, it is intriguing that R1490A/K1491A mutation has little effect on the binding of Mlph-GTBDP to Myo5a tail containing the GTD dimer.

The Mlph-GTBDP binding site in the GTD dimer is not exposed, preventing the binding of Mlph-GTBDP to the GTD. Thus, the Mlph-GTBDP binding site in the GTD dimer must be exposed prior to the binding of Mlph-GTBDP. Therefore, we propose that there are two states of the inhibited Myo5a, *i.e.* the folded state and the preactivated state (Fig. 6). In the folded state, the two GTDs form a head to head dimer via the interaction between the N-terminal extension in one GTD and the Mlph-GTBDP binding site in the counterpart GTD, and interact with the two heads of Myo5a, thus forming a folded, triangular conformation. The preactivated state is similar to the folded state, except that the Mlph-GTBDP binding sites in the GTDs are exposed. Mlph-GTBDP is able to bind to the GTD of Myo5a in the preactivated state, and this binding allosterically inhibits the binding of GTD to the head, thus inducing the extended conformation of Myo5a (Fig. 6).

The binding and activation of Myo5a by Mlph-GTBDP can be illustrated in following reaction,

$$E \underset{k_{-1}}{\overset{k_{+1}}{\rightleftharpoons}} E' \underset{k_{-2}}{\overset{k_{+2}[L]}{\rightleftharpoons}} EL \qquad \text{(Eq. 1)}$$

where E is Myo5a in the folded state, E' is Myo5a in the preactivated state; L is Mlph-GTBDP; and EL is the Myo5a·Mlph-GTBDP complex in the activated, extended state.

The equilibrium of Myo5a in those three states is governed by the rates of each reaction steps. At steady state, the ratio of the concentration of Myo5a·Mlph-GTBDP complex (*EL*) *versus* the total concentration of Myo5a (E_{total}) can be calculated with following equation.

$$\frac{[EL]}{[E_{total}]} = \frac{[L]}{\frac{(k_{+1}+k_{-1})k_{-2}}{k_{+1}k_{+2}} + [L]} \qquad \text{(Eq. 2)}$$

Thus, the apparent dissociation constant K_d is as follows.

$$\frac{(k_{+1}+k_{-1})k_{-2}}{k_{+1}k_{+2}} \qquad \text{(Eq. 3)}$$

In the case of Myo5a-FL, multiple intramolecular interactions, including the head-GTD interaction, stabilize the GTD-GTD interaction, rendering most molecules in the folded state. Thus, $k_{+1} \ll k_{-1}$ and $K_d \approx k_{-1}k_{-2}/k_{+1}k_{+2}$. R1490A/K1491A mutation weakens the GTD-GTD interaction, thus increasing k_{+1} and decreasing K_d. Therefore, R1490A/K1491A mutation enhances the binding of Myo5a-FL to Mlph-GTBDP.

On the other hand, in the case of Myo5a tail, such as His-Myo5a-T1344, lacking of the head-GTD interaction weakens the GTD-GTD interaction, thus increasing k_{+1} and decreasing k_{-1}. It is possible that, in the case of His-Myo5a-T1344, $k_{+1} \gg k_{-1}$ and $K_d \approx k_{-2}/k_{+2}$. Therefore, although R1490A/K1491A mutation further weakens the GTD-GTD interaction and increases k_{+1}, K_d is not changed. Thus, R1490A/K1491A mutation has little effect on the binding of His-Myo5a-T1344 to Mlph-GTBDP.

In addition to the GTBD, Mlph contains another Myo5a-binding site, the EFBD, which binds to the exon F encoded region in the tail of Myo5a. We previously have shown that Mlph construct containing both the GTBD and the EFBD has higher affinity to Myo5a than the GTBD alone (15). If our pro-

posed mechanism is correct, it is possible that the binding of EFBD to the exon F region weakens the GTD-GTD interaction, thus facilitating the formation of preactivated state of Myo5 and enhancing the GTBD binding. Further experiments are needed to clarify this issue.

Author Contributions—W.-B .Z. and L.-L. Y. performed experiments. W.-B. Z. and X.-D. L. designed research and analyzed the data. X.-D. L. conceived the project and wrote the manuscript. All authors reviewed the manuscript.

References

1. Cheney, R. E., O'Shea, M. K., Heuser, J. E., Coelho, M. V., Wolenski, J. S., Espreafico, E. M., Forscher, P., Larson, R. E., and Mooseker, M. S. (1993) Brain myosin-V is a two-headed unconventional myosin with motor activity. *Cell* **75,** 13–23
2. Rodriguez, O. C., and Cheney, R. E. (2002) Human myosin-Vc is a novel class V myosin expressed in epithelial cells. *J. Cell Sci.* **115,** 991–1004
3. Zhao, L. P., Koslovsky, J. S., Reinhard, J., Bähler, M., Witt, A. E., Provance, D. W., Jr., and Mercer, J. A. (1996) Cloning and characterization of myr 6, an unconventional myosin of the dilute/myosin-V family. *Proc. Natl. Acad. Sci. U.S.A.* **93,** 10826–10831
4. Wang, F., Thirumurugan, K., Stafford, W. F., Hammer, J. A., 3rd, Knight, P. J., and Sellers, J. R. (2004) Regulated conformation of myosin V. *J. Biol. Chem.* **279,** 2333–2336
5. Li, X. D., Mabuchi, K., Ikebe, R., and Ikebe, M. (2004) Ca^{2+}-induced activation of ATPase activity of myosin Va is accompanied with a large conformational change. *Biochem. Biophys. Res. Commun.* **315,** 538–545
6. Krementsov, D. N., Krementsova, E. B., and Trybus, K. M. (2004) Myosin V: regulation by calcium, calmodulin, and the tail domain. *J. Cell Biol.* **164,** 877–886
7. Li, X. D., Jung, H. S., Wang, Q., Ikebe, R., Craig, R., and Ikebe, M. (2008) The globular tail domain puts on the brake to stop the ATPase cycle of myosin Va. *Proc. Natl. Acad. Sci. U.S.A.* **105,** 1140–1145
8. Thirumurugan, K., Sakamoto, T., Hammer, J. A., 3rd, Sellers, J. R., and Knight, P. J. (2006) The cargo-binding domain regulates structure and activity of myosin 5. *Nature* **442,** 212–215
9. Liu, J., Taylor, D. W., Krementsova, E. B., Trybus, K. M., and Taylor, K. A. (2006) Three-dimensional structure of the myosin V inhibited state by cryoelectron tomography. *Nature* **442,** 208–211
10. Li, X. D., Jung, H. S., Mabuchi, K., Craig, R., and Ikebe, M. (2006) The globular tail domain of myosin Va functions as an inhibitor of the myosin Va motor. *J. Biol. Chem.* **281,** 21789–21798
11. Wang, Z., Edwards, J. G., Riley, N., Provance, D. W., Jr., Karcher, R., Li, X. D., Davison, I. G., Ikebe, M., Mercer, J. A., Kauer, J. A., and Ehlers, M. D. (2008) Myosin Vb mobilizes recycling endosomes and AMPA receptors for postsynaptic plasticity. *Cell* **135,** 535–548
12. Yao, L. L., Shen, M., Lu, Z., Ikebe, M., and Li, X. D. (2016) Identification of the isoform-specific interactions between the tail and the head of class V myosin. *J. Biol. Chem.* **291,** 8241–8250
13. Wu, X. S., Rao, K., Zhang, H., Wang, F., Sellers, J. R., Matesic, L. E., Copeland, N. G., Jenkins, N. A., and Hammer, J. A., 3rd (2002) Identification of an organelle receptor for myosin-Va. *Nat. Cell Biol.* **4,** 271–278
14. Fukuda, M., and Kuroda, T. S. (2004) Missense mutations in the globular tail of myosin-Va in dilute mice partially impair binding of Slac2-a/melanophilin. *J. Cell Sci.* **117,** 583–591
15. Li, X. D., Ikebe, R., and Ikebe, M. (2005) Activation of myosin Va function by melanophilin, a specific docking partner of myosin Va. *J. Biol. Chem.* **280,** 17815–17822
16. Geething, N. C., and Spudich, J. A. (2007) Identification of a minimal myosin Va binding site within an intrinsically unstructured domain of melanophilin. *J. Biol. Chem.* **282,** 21518–21528
17. Fukuda, M., and Itoh, T. (2004) Slac2-a/melanophilin contains multiple PEST-like sequences that are highly sensitive to proteolysis. *J. Biol. Chem.* **279,** 22314–22321
18. Yao, L. L., Cao, Q. J., Zhang, H. M., Zhang, J., Cao, Y., and Li, X. D. (2015) Melanophilin stimulates myosin-5a motor function by allosterically inhibiting the interaction between the head and tail of myosin-5a. *Sci. Rep.* **5,** 10874
19. Wei, Z., Liu, X., Yu, C., and Zhang, M. (2013) Structural basis of cargo recognitions for class V myosins. *Proc. Natl. Acad. Sci. U.S.A.* **110,** 11314–11319
20. Pylypenko, O., Attanda, W., Gauquelin, C., Lahmani, M., Coulibaly, D., Baron, B., Hoos, S., Titus, M. A., England, P., and Houdusse, A. M. (2013) Structural basis of myosin V Rab GTPase-dependent cargo recognition. *Proc. Natl. Acad. Sci. U.S.A.* **110,** 20443–20448
21. Lu, Z., Shen, M., Cao, Y., Zhang, H. M., Yao, L. L., and Li, X. D. (2012) Calmodulin bound to the first IQ motif is responsible for calcium-dependent regulation of myosin 5a. *J. Biol. Chem.* **287,** 16530–16540
22. Nascimento, A. F., Trindade, D. M., Tonoli, C. C., de Giuseppe, P. O., Assis, L. H., Honorato, R. V., de Oliveira, P. S., Mahajan, P., Burgess-Brown, N. A., von Delft, F., Larson, R. E., and Murakami, M. T. (2013) Structural insights into functional overlapping and differentiation among myosin V motors. *J. Biol. Chem.* **288,** 34131–34145
23. Velvarska, H., and Niessing, D. (2013) Structural insights into the globular tails of the human type v myosins Myo5a, Myo5b, and Myo5c. *PLoS One* **8,** e82065
24. Spudich, J. A., and Watt, S. (1971) The regulation of rabbit skeletal muscle contraction. I. Biochemical studies of the interaction of the tropomyosin-troponin complex with actin and the proteolytic fragments of myosin. *J. Biol. Chem.* **246,** 4866–4871
25. Seperack, P. K., Mercer, J. A., Strobel, M. C., Copeland, N. G., and Jenkins, N. A. (1995) Retroviral sequences located within an intron of the dilute gene alter dilute expression in a tissue-specific manner. *EMBO J.* **14,** 2326–2332
26. Donovan, K. W., and Bretscher, A. (2015) Head-to-tail regulation is critical for the in vivo function of myosin V. *J. Cell Biol.* **209,** 359–365